

# Silicon Carbide Micro-reaction-sintering Using A Multilayer Silicon Mold

Shinya Sugimoto<sup>1</sup>, Shuji Tanaka<sup>1</sup>, Jing-Feng Li<sup>2</sup>, Ryuzo Watanabe<sup>2</sup> and Masayoshi Esashi<sup>3</sup>

<sup>1</sup>Department of Mechatronics and Precision Engineering, Tohoku University

<sup>2</sup>Department of Materials Processing, Tohoku University

<sup>3</sup>New Industry Creation Hatchery Center, Tohoku University

Aza-Aoba, Aramaki, Aoba-ku, Sendai 980-8579, Japan.

e-mail: sugimoto@mems.mech.tohoku.ac.jp

## ABSTRACT

This paper describes a novel process, “Silicon Carbide Micro-reaction-sintering”, to fabricate high-aspect-ratio silicon carbide microstructures. This process consists of micromachining of silicon molds, filling of material powders ( $\alpha$ -silicon carbide, graphite, silicon and phenol resin) into the molds, bonding of the molds with adhesive and reaction-sintering by hot isostatic pressing (HIP). Using our process, we have successfully fabricated silicon carbide microrotors of 5 and 10 mm diameters for micromachined gas turbines. We observed the cross section of the microrotors with a scanning electron microscope (SEM). The SEM observation demonstrated that the material powder was densely reaction-sintered by HIP. We also investigated the compositions of the microrotors by X-ray diffraction (XRD) analysis. The XRD analyses proved that graphite in the material powder reacted with melted silicon derived from the mold, and consequently  $\beta$ -silicon carbide was produced around the  $\alpha$ -silicon carbide originally included in the material powder.

## INTRODUCTION

Silicon carbide (SiC) has outstanding properties of heat resistance, wear resistance, chemical inertness and high hardness. These properties are attractive for microelectromechanical systems (MEMS) in harsh environments, such as fuel nozzles of heat engines, microthrusters for small spacecrafts and micro-gas turbines [1]. Among them, the SiC micromachined gas turbine requires especially challenging developments.

We are developing the SiC micromachined gas turbine, which has a microrotor of 5-10 mm diameters with high-aspect-ratio blades on the both sides. It is, however, difficult to fabricate such a microrotor using conventional methods. For example, grinding and electric discharge machining (EDM) have the limitation of shape resolution due to the large size of tools. They also suffer from the rapid wear of tools especially in the case of using microtools. Chemical vapor deposition

(CVD) and reactive ion etching (RIE) realize shape resolution of micrometer order. However, they generally suffer from slow fabrication speed of less than several micrometers per hour, so that they require impractically-long time to fabricate SiC microstructures of more than several ten micrometers in height.

Therefore, we have developed a novel microfabrication process, “SiC Micro-reaction-sintering”, combining silicon micromachining, reaction-sintering and lost-mold technique [2] to form up-to-millimeter-sized SiC microstructures with shape resolution of micrometer order [3].

## PROPOSAL OF SILICON CARBIDE MICRO-REACTION-SINTERING PROCESS

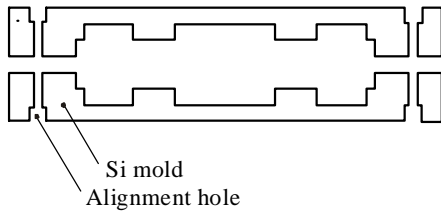
The SiC micro-reaction-sintering process is summarized as reaction-sintering of material powder including SiC, graphite and silicon (Si) filled in micromachined Si molds by hot isostatic pressing (HIP). Figure 1 illustrates the SiC micro-reaction-sintering process using 2-layer Si molds. The process consists of 9 steps; (1) micromachining of Si molds, (2)(3) filling of material powders into the molds, (4)(5) bonding of the molds, (6)(7) preparation of reaction-sintering, (8) reaction-sintering by HIP and (9) release of the sintered workpiece from the molds. The detail of each step, whose number corresponds with that in Fig. 1, is as follows.

(1) Si molds for reaction-sintering are fabricated by photolithography and deep-RIE. The molds have alignment holes, which are used in the step (5).

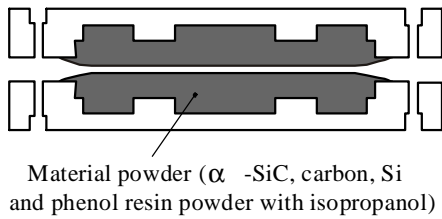
(2) Material powder is prepared by mixing  $\alpha$ -silicon carbide ( $\alpha$ -SiC), graphite, Si, binder (phenol resin) and small solvent (isopropanol), and is filled into the molds.

(3) Cold isostatic pressing (CIP) is performed to pack the material powder into the molds; the molds with the material powder are wrapped in rubber bags, and are isostatically pressed by hydrostatic pressure of several hundred atmospheres at room temperature.

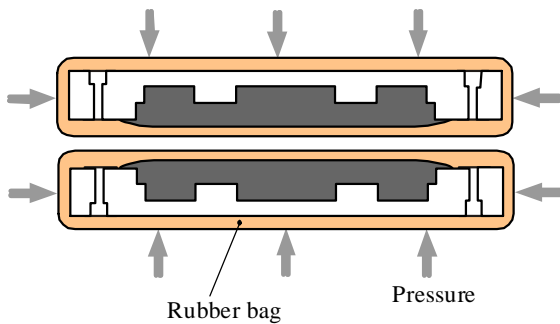
(1) Fabrication of Si molds  
by photolithography and deep-RIE



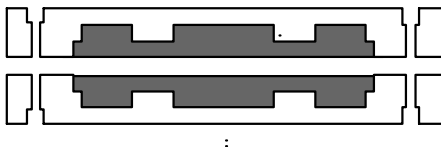
(2) Filling of material powder into the molds



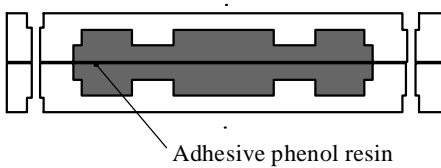
(3) CIP to pack the material powder into the molds



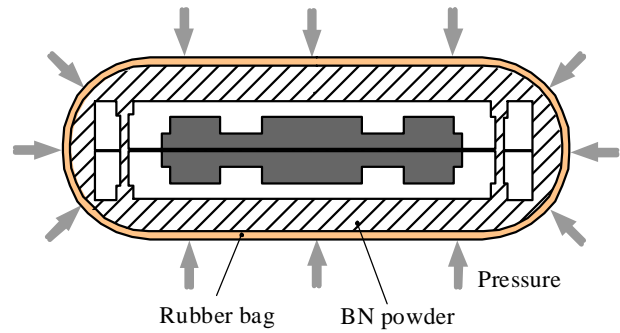
(4) Grinding to flatten the surfaces



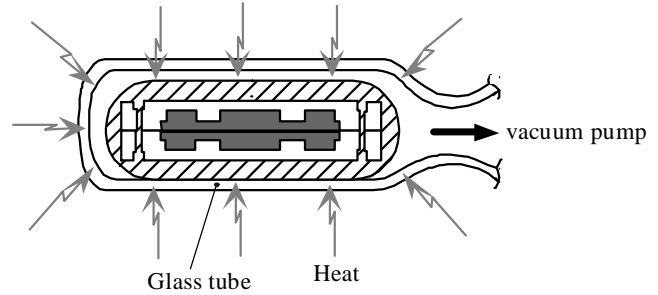
(5) Bonding the molds with adhesive phenol resin



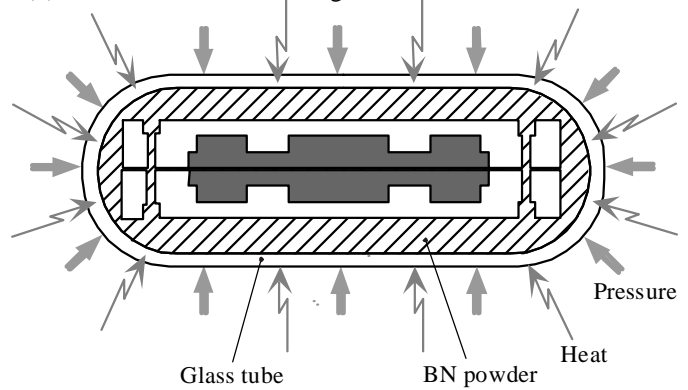
(6) CIP to wrap the sample in BN powder



(7) Glass-encapsulation in vacuum



(8) HIP for reaction-sintering



(9) Release of the sample by wet etching

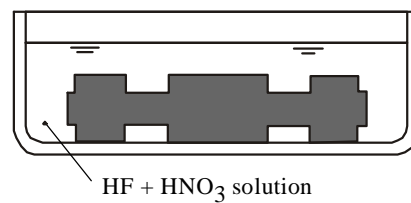


Fig. 1: Schematic of the SiC micro-reaction-sintering process.

(4) The surfaces of the molds are finished to be flat by grinding away the excess material powder on the molds.

(5) The molds with the material powder are aligned each other by observing the alignment holes with an optical microscope, and are bonded with adhesive (phenol resin with isopropanol).

(6) CIP is performed again to wrap the bonded mold in boron nitride (BN) powder to prevent the mold from reacting with a glass tube in the step (8).

(7) The mold wrapped in the BN powder is vacuum-encapsulated in a glass tube.

(8) The material powder in the mold is reaction-sintered by HIP; the material powder in the mold is isostatically pressed by argon pressure of more than several hundred atmospheres, at higher temperature of more than the melting point of Si ( $1414^{\circ}\text{C}$ ). The melted silicon derived from the mold penetrates into the material powder, and reacts with graphite in the material powder to become SiC. The new SiC grows around the original  $\alpha$ -SiC powder, so that a densely-sintered SiC is obtained. On the bonding surface, the carbonized phenol resin also reacts with the melted silicon to become SiC, and consequently the originally-separated parts of the material powder are completely bonded to become a single sintered body without the bonding surface.

(9) The Si mold covering the sintered workpiece is etched away by etchant composed of hydrofluoric acid and nitric acid.

This process has two advantages. The first advantage is that photolithography and deep-RIE can fabricate precisely the Si mold with high-aspect-ratio microstructures. The second advantage is that SiC microparts with complicated multilayer structures can be formed easily by bonding the molds only with the adhesive. The process illustrated in Fig. 1 can be also applied to the process using more than three molds.

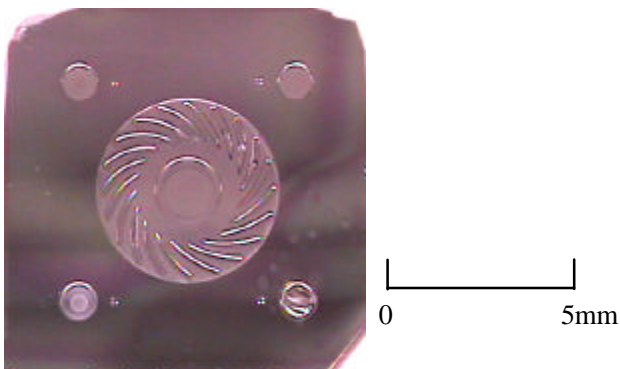


Fig. 2: A photograph of the Si mold for a gas turbine of 5 mm diameter.

## EXPERIMENTAL MICROFABRICATION OF SILICON MOLDS

We used this process, “ Micro-reaction-sintering ”, to fabricate a microrotor for a micromachined gas turbine. The microrotor has a complicated multilayer structure with a compressor and a turbine on the upper and lower side respectively. To form the microrotor, a pair of Si molds, a mold for the compressor side and that for the turbine side, is used. Figure 2 shows a photograph of a Si mold for the turbine side, whose size is  $10 \times 10 \times 0.6 \text{ mm}^3$ . Using this mold and a mold for the compressor side, we have formed a microrotor of 5 mm diameter and  $800 \text{ }\mu\text{m}$  thickness. The process to fabricate the Si mold proceeds along the following steps, whose numbers correspond with those in Fig. 3.

(1) An oxide film is thermally grown on both sides of a  $600\text{-}\mu\text{m}$ -thick Si substrate. Positive photoresist (PR) is formed on the upper side of the substrate by spin-coating, and the oxide film on the lower side is then etched away by buffered hydrofluoric acid (HF).

(2) PR is formed on the lower side by spin-coating, and patterned with the shape of the alignment holes. The substrate is etched by deep-RIE.

(3) The PR on the upper side is patterned with the shape of a disk. The oxide film is etched away by buffered HF.

(4) The PR is removed. A PR is formed again on the upper side and is patterned with the shape of compressor/turbine blades. The substrate is etched by deep-RIE to form a cavity for the blades.

(5) The PR is removed. Using the oxide mask patterned in the step (3), the substrate is etched by deep-RIE to form a cavity for the disk. The alignment holes are penetrated in this step.

(6) The oxide film is etched away by buffered HF.

By applying the similar process to thicker Si substrate, whose size is  $20 \times 20 \times 1.5 \text{ mm}^3$ , we have also prepared Si molds with a cavity of 1 mm depth for a microrotor of 10 mm diameter and 2 mm thickness.

## REACTION-SINTERING

We performed the reaction-sintering three times in the conditions listed in Table 1. In the 1st and 2nd reaction-sintering, material powders with the same compositions were reaction-sintered at different temperatures and pressures. In the 3rd reaction-sintering, material powder with different compositions from the previous one was reaction-sintered at the same temperature and pressure that were used in the 2nd reaction-sintering.  $\alpha$ -SiC powder of  $0.47 \text{ }\mu\text{m}$  in average diameter, graphite powder of  $5 \text{ }\mu\text{m}$ , Si powder of  $1 \text{ }\mu\text{m}$  and phenol resin powder are

used as the material powder. In the preparation of the material powder, these powders with small solvent of isopropanol were mixed into the compositions described in Table 1. The two times of cold isostatic pressing (the step (3) and (6) in Fig. 1) before the reaction-sintering were performed at hydrostatic pressure of 100 MPa and at room temperature for 15 sec. For the vacuum-encapsulation (the step (7) in Fig. 1), a Pyrex glass tube was used.

Figure 4 (a) and (b) are photographs of microrotors fabricated by the 1st and 2nd reaction-sintering respectively. As shown in Fig. 4, the shape of the Si mold was transferred precisely to that of the sintered microrotor. Figure 4 (b-2), which shows the cross section of the microrotor, indicates that the bonding surface

disappeared. The shrinkage of the sintered rotors compared to the molds was estimated at about 3% by measuring the diameters of the molds and the sintered microrotors using an optical microscope.

Figure 5 (a), (b) and (c) are scanning electron micrographs (SEMs) of the cross sections of the microrotors formed by the 1st, 2nd and 3rd reaction-sintering respectively. Figure 5 (a) shows grains of 1-4  $\mu\text{m}$  diameters. We think that the grains are the material powders which remain not to be reaction-sintered. The cross section shown in Fig. 5 (b) is finer than that shown in Fig. 5 (a). The HIP condition of the 2nd reaction-sintering proves to be better than that in the 1st reaction-sintering, because the compositions of the material powder used in the both reaction-sintering are the same.

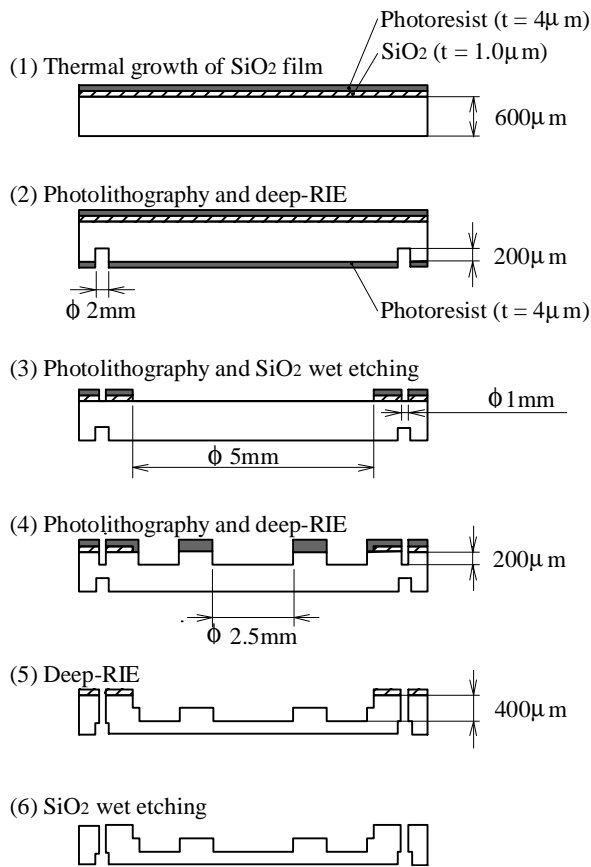


Fig. 3: Process flow to fabricate the Si molds.

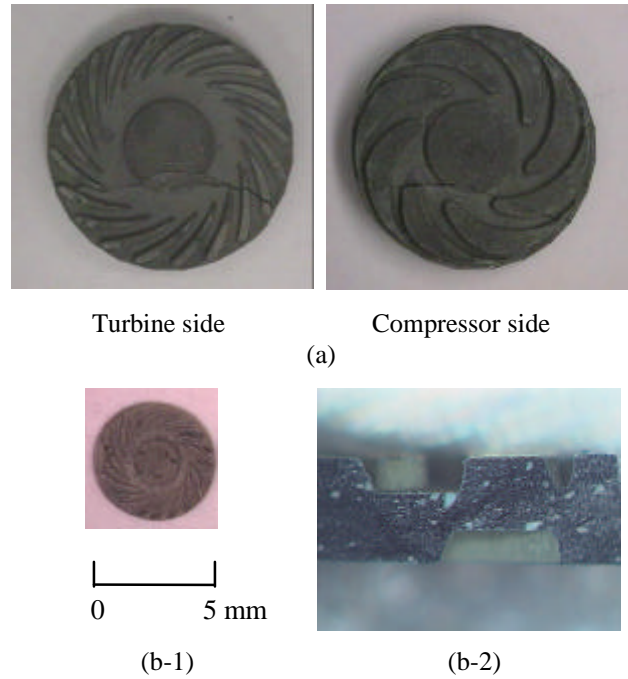


Fig. 4: Photographs of (a) the microrotor of 10 mm diameter formed by the 1st reaction-sintering, (b-1) the microrotor of 5 mm diameter and (b-2) the cross section of the rotor formed by the 2nd reaction-sintering.

Table 1: Conditions of reaction-sintering

Experiment number	1st	2nd	3rd
Compositions of material powder	$\alpha$ -SiC : 3.0g Graphite : 1.5g Phenol resin : 0.45g	$\alpha$ -SiC : 3.0g Graphite : 1.5g Phenol resin : 0.45g	Si : 2.8g Graphite : 1.2g Phenol resin : 0.36g
Furnace temperature ( °C )	1500 (15 °C /min*)	1700 (17 °C /min*)	1700 (17 °C /min*)
Furnace pressure (MPa)	100	50	50
Rotor diameter of the Si mold	$\phi$ 10mm	$\phi$ 5mm	$\phi$ 5mm

(\* Heating speed of the furnace)

Figure 5 (c) shows a rougher cross section with grains of 1-5  $\mu\text{m}$  diameters than that shown in Fig. 5 (b). The compositions of the material powder used in the 2nd reaction-sintering proves to be better than that used in the 3rd reaction-sintering, because the HIP conditions of the both reaction-sintering are the same. Therefore, we can conclude that the condition of the 2nd reaction-sintering was the best in these experiments.

### X-RAY DIFFRACTION ANALYSES

We have investigated the compositions of the sintered samples by X-ray diffraction (XRD) analysis. Figure 6, 7 and 8 show the XRD patterns of the samples obtained by the 1st, 2nd and 3rd reaction-sintering respectively. Each figure shows the XRD patterns of (a) the material powder and (b) the sintered sample. The marks ( $\triangle$ ,  $\square$ ,  $\circ$ ,  $\bullet$ ) represent the materials which have the peaks of XRD (graphite, Si,  $\alpha$ -SiC,  $\beta$ -SiC). Graphite, Si and  $\alpha$ -SiC have high peaks at  $2\theta = 26.5$ ,  $28.0$  and  $36.0^\circ$  respectively.  $\beta$ -SiC has a high peak at  $2\theta = 41.0^\circ$ , by which  $\beta$ -SiC can be distinguished from  $\alpha$ -SiC. For example, Fig. 6 (a) has the peaks of graphite and  $\alpha$ -SiC, and Fig. 6 (b) has the peaks of graphite,  $\alpha$ -SiC and  $\beta$ -SiC.

As shown in Fig. 6, the peaks of graphite decreased and the peaks of  $\beta$ -SiC appeared after the 1st reaction-sintering. This result demonstrates that graphite in the material powder reacted with melted silicon derived from the mold to become  $\beta$ -SiC in the reaction-sintering. A certain amount of graphite, however, remained in the sintered sample, suggesting imperfect reaction-sintering.

Fig. 7 indicates that the peaks of graphite disappeared and the peaks of  $\beta$ -SiC appeared after the 2nd reaction-sintering. This result suggests that most of the graphite in the material powder contributed to the reaction-sintering.

Fig. 8 indicates that the peaks of graphite and Si disappeared and the peaks of  $\beta$ -SiC appeared after the 3rd sintering. This result demonstrates that  $\beta$ -SiC is produced by the reaction of graphite and melted silicon.

From the results of the XRD analyses and the SEM observations, we can conclude again that the condition of the 2nd reaction-sintering is the best in these experiments. We think that high temperature of  $1700^\circ\text{C}$  promoted the penetration of melted silicon into the material powder as well as the reaction of graphite and melted silicon into  $\beta$ -SiC, so that  $\beta$ -SiC completely filled the space among  $\alpha$ -SiC originally-included in the material powder in the 2nd reaction-sintering.

### CONCLUSIONS

We have developed a novel process, "Silicon Carbide Micro-reaction-sintering", to fabricate high-aspect-ratio SiC microstructures using micromachined Si molds. This process consists of micromachining of Si molds, filling of material powder ( $\alpha$ -SiC, graphite, Si and phenol resin with isopropanol) into the molds, bonding of the molds with adhesive and reaction-sintering by hot isostatic pressing (HIP).

Using our process, we have successfully formed micro-rotors of 5 and 10 mm diameters for micromachined gas turbines. The microrotor has compressor blades and turbine blades on each side respectively. We have confirmed that the shape of the Si mold was transferred precisely to that of the sintered microrotor. We have also confirmed  $\beta$ -SiC was produced by the reaction of graphite originally-included in the material powder with Si of the mold by X-ray diffraction analysis.

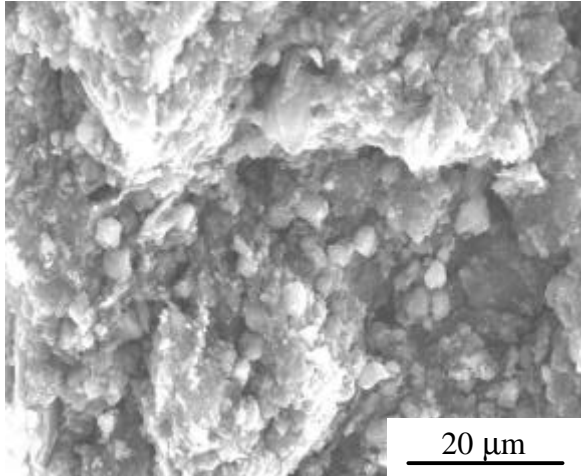
We believe that this process can open up the way to new applications of SiC in the area of micromachines, such as a micromachined gas turbine, a microrocket thruster, a fuel nozzle and so on.

### ACKNOWLEDGMENTS

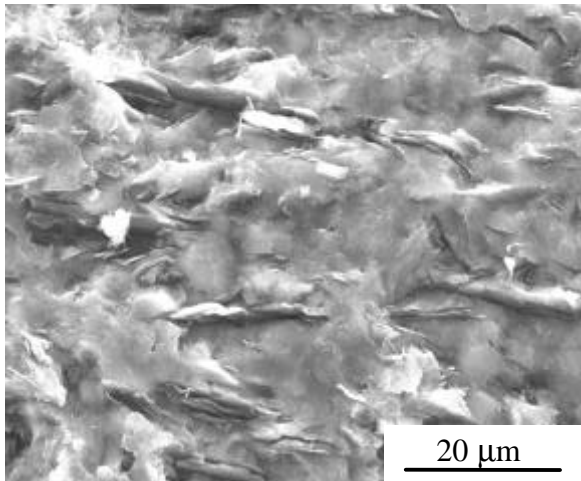
This work was supported by the Japan Society for the Promotion of Science (Research for the Future Program: Project No. 96P00802) and Yamagata Prefecture (Micromachine Research and Development Project). We used Venture Business Laboratory, Tohoku University to fabricate Si molds.

### REFERENCES

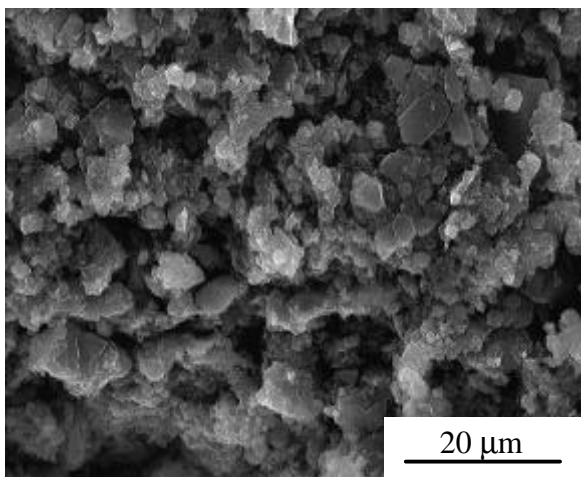
- [1] A.H. Epstein, et al., "Micro-Heat Engines, Gas Turbines, and Rocket Engines -The MIT Microengine Project-", Proc. 28th AIAA Fluid Dynamics Conference, 4th AIAA Shear Flow Control Conference, June 29, July 2, 1997, AIAA paper 97-1773, Snowmass Village, CO, USA.
- [2] S. Wang, J. Li, X. Li and M. Masayoshi, "Processing of PZT Microstructures", Sensors and Materials, Vol.10, No.6, 1998, pp.375-384.
- [3] S. Tanaka, S. Sugimoto, J.F. Li, R. Watanabe and M. Esashi, "Silicon Carbide Micro-reaction-sintering Using Micromachined Silicon Molds", submitted to J. Micro-electromechanical Systems.



(a)



(b)



(c)

Fig. 5: Scanning electron micrographs of the cross sections of the microrotors formed in the (a) 1st, (b) 2nd and (c) 3rd reaction-sintering.

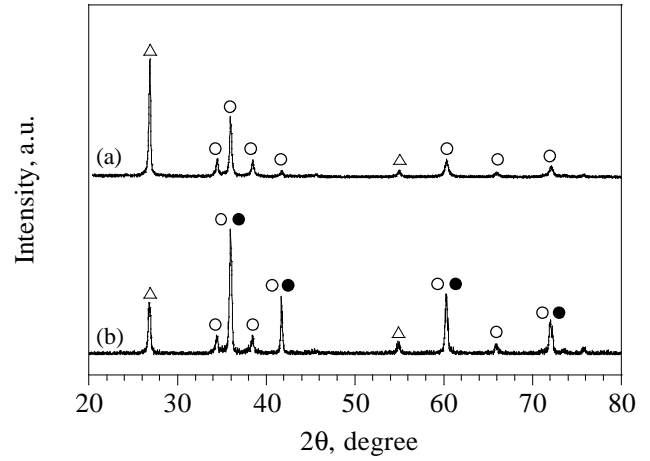


Fig. 6: XRD patterns of (a) the material powder and (b) the sintered workpiece obtained by the 1st reaction-sintering. The marks ( $\Delta$ ,  $\circ$ ,  $\bullet$ ) represent the materials (graphite,  $\alpha$ -SiC,  $\beta$ -SiC).

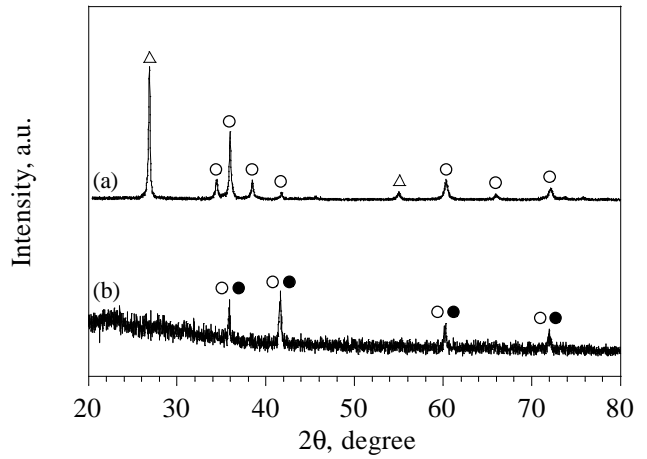


Fig. 7: XRD patterns of (a) the material powder and (b) the sintered workpiece obtained by the 2nd reaction-sintering. The marks ( $\Delta$ ,  $\circ$ ,  $\bullet$ ) represent the (graphite,  $\alpha$ -SiC,  $\beta$ -SiC).

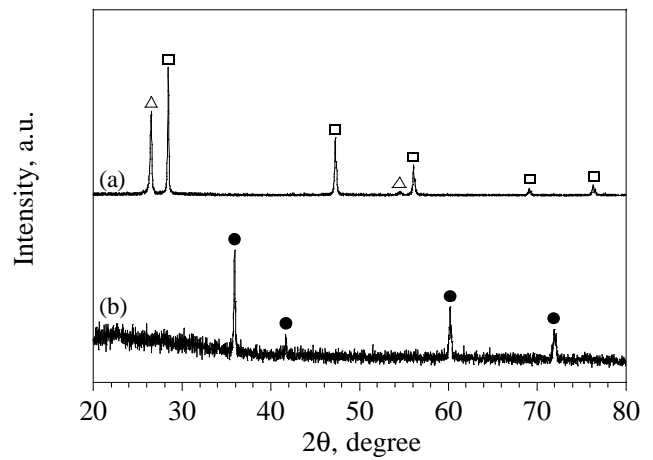


Fig. 8: XRD patterns of (a) the material powder and (b) the sintered workpiece obtained by the 3rd reaction-sintering. The marks ( $\Delta$ ,  $\square$ ,  $\bullet$ ) represent the materials (graphite, Si,  $\beta$ -SiC).